

Novel Platinum(IV)–Carbohydrate Complexes: Metal Ion Coordination Behavior of Monosaccharides in Organic Solvents

Henrik Junicke,[†] Clemens Bruhn,[†] Ralph Kluge,[‡] Anthony S. Serianni,[§] and Dirk Steinborn^{*,†}

Contribution from the Institut für Anorganische Chemie and Institut für Organische Chemie, Martin-Luther-Universität Halle-Wittenberg, Kurt-Mothes Strasse 2, D-06120 Halle/Saale, Germany, and Department of Chemistry and Biochemistry, University of Notre Dame, Notre Dame, Indiana 46556-5670

Received January 27, 1999

Abstract: New platinum(IV)-coordinated carbohydrate complexes [PtMe₃L]BF₄ (**14E**–**21E**, **22D**–**24D**) have been prepared from the reaction of [PtMe₃(Me₂CO)₃]BF₄ (**1**) with a wide range of isopropylidene-protected carbohydrates L' in acetone. These complexation reactions can be accompanied by a platinum-promoted cleavage of an isopropylidene group (**14E**, L' = 1,2;5,6-di-*O*-isopropylidene- α -D-glucofuranose (**1A**), L = 1,2-*O*-isopropylidene- α -D-glucofuranose; **15E**, L' = 3-*O*-acetyl-1,2;5,6-di-*O*-isopropylidene- α -D-glucofuranose (**2A**), L = 3-*O*-acetyl-1,2-*O*-isopropylidene- α -D-glucofuranose; **16E**, L' = 3-*O*-(methylsulfonyl)-1,2;5,6-di-*O*-isopropylidene- α -D-glucofuranose (**3A**), L = 3-*O*-(methylsulfonyl)-1,2-*O*-isopropylidene- α -D-glucofuranose; **17E**, L' = 1,2;5,6-di-*O*-isopropylidene- α -D-allofuranose (**4A**), L = 1,2-*O*-isopropylidene- α -D-allofuranose; **18E**, L' = 2,3;4,6-di-*O*-isopropylidene-2-keto-L-gulonic acid (**5A**), L = 2,3-*O*-isopropylidene-2-keto-L-gulonic acid; **19E**, L' = 2,3;4,6-di-*O*-isopropylidene- α -L-sorbofuranose (**6A**), L = 2,3-*O*-isopropylidene- α -L-sorbofuranose). In some cases, complexation proceeds without the loss of an isopropylidene group (**14E**, L = L' = 1,2-*O*-isopropylidene- α -D-glucofuranose (**10B**); **15E**, L = L' = 3-*O*-acetyl-1,2-*O*-isopropylidene- α -D-glucofuranose (**11B**); **20E**, L = L' = 1,2-*O*-isopropylidene- α -D-xylofuranose (**12B**), **21E**, L = L' = 5,6-*O*-isopropylidene-D-gulono- γ -lactone (**13B**)). Furthermore, complexes **22D**–**24D** with diprotected carbohydrate ligands undergo a platinum-promoted cleavage of an isopropylidene group in wet methylene chloride to give **19E**, cleavage of the carbohydrate ligand L (**7A**) to give [PtMe₃(H₂O)₃]BF₄, and substitution of the isopropylidene ligand by an aqua ligand to give [PtMe₃L(H₂O)]BF₄ (**24D'**, L = 2,3;4,5-di-*O*-isopropylidene- β -D-fructopyranose), respectively. Complex **14E** reacted in acetone within 1 week in a platinum-promoted addition of an isopropylidene protecting group, yielding [PtMe₃L']BF₄ (**25D**, L' = 1,2;5,6-di-*O*-isopropylidene- α -D-glucofuranose). The results show that carbohydrates can act as tridentate neutral ligands with a wide variety of donor sites: 3 \times OH (**14E**, **17E**–**19E**), 2 \times OH + O_{COMe} (**15E**), 2 \times OH + O_{SO₂Me} (**16E**), 2 \times OH + O_{ring} (**20E**), 2 \times OH + O_{acetal} (**21E**), 1 \times OH + O_{ring} + O_{acetal} (**22D**–**25D**). Bidentate ligation (OH + O_{ring}) is observed in **24D'**. Complexes **14E** singly ¹³C-labeled at each of the saccharide carbons were prepared, and an analysis of the *J* couplings involving the labeled carbons permitted an assignment of the solution conformation of the carbohydrate ligand. X-ray structure analysis of **19E** (monoclinic, *P*2₁, *a* = 8.607(3) Å, *b* = 9.955(4) Å, *c* = 11.415(4) Å, *Z* = 2) and **24D'** (orthorhombic, *P*2₁2₁2₁, *a* = 9.851(2) Å, *b* = 11.141(4) Å, *c* = 20.418(6) Å, *Z* = 4) exhibits the same coordination in the solid state as in solution, namely, via the three hydroxyl groups, yielding a strained-cyclic system (**19E**) and a five-membered 1,3,2-dioxaplatina ring (**24D'**).

Introduction

The metal-binding properties of carbohydrates have been shown to be of fundamental importance in many biochemical processes such as the transport and storage of metals,^{1,2} the function and regulation of metalloenzymes, the mechanism of action of metal-containing pharmaceuticals, and toxic metal metabolism.³ Although coordination chemistry plays a central

role in these processes, carbohydrate–metal complexes are still poorly understood; relatively few well-characterized complexes of transition metals with carbohydrate ligands have been reported,⁴ especially those lacking anchor groups. In recent years, the bioinorganic chemistry of heavy metal–carbohydrate complexes has been investigated to understand redox systems with metal ions in higher oxidation states⁵ and to understand the complexation behavior of metals with carbohydrate polymers such as cellulose or cyclodextrins.⁶ In the case of platinum, the synthesis and application of platinum compounds in chemotherapy⁷ has received considerable attention because of their

* To whom correspondence should be addressed.

[†] Institut für Anorganische Chemie, Martin-Luther-Universität Halle-Wittenberg.

[‡] Institut für Organische Chemie, Martin-Luther-Universität Halle-Wittenberg.

[§] University of Notre Dame.

(1) Sauchelli, V. *Trace Elements in Agriculture*; Van Nostrand: New York, 1969; p 248.

(2) Holm, R. H.; Berg, J. M. *Pure Appl. Chem.* **1984**, *56*, 1645–1657.

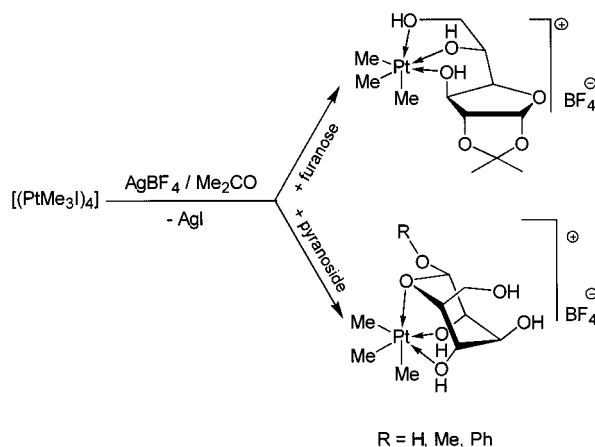
(3) Predki, P. F.; Whitfield, D. M.; Sarker, B. *Biochem. J.* **1992**, *281*, 835–841.

(4) a) Piarulli, U.; Floriani, C. *Prog. Inorg. Chem.* **1997**, *45*, 393–429. (b) Burger, J.; Gack, C.; Klüfers, P. *Angew. Chem.* **1995**, *107*, 2950–2951; *Angew. Chem., Int. Ed. Engl.* **1995**, *34*, 2647–2649.

(5) Geisselmann, A.; Klüfers, P.; Pilawa, B. *Angew. Chem.* **1998**, *110*, 1181–1184; *Angew. Chem., Int. Ed. Engl.* **1998**, *37*, 1119–1121.

(6) Brenner, K.; Klüfers, P.; Schuhmacher, J. *Angew. Chem.* **1997**, *109*, 783–785; *Angew. Chem., Int. Ed. Engl.* **1997**, *36*, 743–745.

Scheme 1



lower toxicity and the possibility of oral administration. The synthesis of platinum(IV)–carbohydrate complexes is complicated by the high oxidation state of the metal ion and the reduction potential of the carbohydrate. Additionally, in aqueous solution, metal ions coordinate with water molecules, and the un-ionized hydroxyl groups of carbohydrates are weak competitors for metal ion coordination under these conditions. Therefore, complexes with functionalized and deprotonated carbohydrate ligands are more common.⁸

Recently we synthesized and characterized the first platinum(IV) complexes with neutral, nonfunctionalized monosaccharides lacking anchor groups (Scheme 1) using a platinum trimethyltris(acetone) complex suitable for substitution reactions with weak donor ligands such as nondeprotonated carbohydrates.^{9,10} The carbohydrates serve as *facial* coordinating tridentate ligands either with three OH group donors contributed by furanosyl rings or with two OH group and one acetal oxygen donors contributed by pyranosyl rings.

In this paper we demonstrate the significant versatility in the coordination of neutral carbohydrate ligands to platinum(IV) and describe the platinum-promoted addition and cleavage of isopropylidene protecting groups. Furthermore, we describe the effect of platinum coordination on the conformation of the carbohydrate ligand in nonaqueous solution by NMR using ¹³C-labeled ligands, ESI-MS, and X-ray crystallography.

Experimental Section

Materials and General Procedures. NMR spectra were obtained on Varian UNITY Plus 600 and Varian VXR-500S spectrometers at the University of Notre Dame (USA) and on the UNITY 500 and Gemini 2000 spectrometers at the Martin-Luther-Universität Halle-

(7) (a) *Metal Complexes in Cancer Chemotherapy*; Keppler, B. K., Ed.; VCH: Weinheim, 1993. (b) *Molecular Aspects of Anticancer Drug–DNA Interactions*; Neidle, S., Waring, M., Eds.; Macmillan: Basingstoke U.K., 1993; Vol. 2. (c) Comess, K. M.; Lippard, S. J. Reference 7b, pp 134–168. (d) McKeage, M. J.; Kelland, L. R. Reference 7b, pp 169–212.

(8) (a) Nagel, Y.; Beck, W. Z. *Naturforsch. B* **1985**, *40*, 1181–1187. (b) Tsubomura, T.; Yano, S.; Kobayashi, K.; Sakurai, T.; Yoshikawa, S. J. *Chem. Soc., Chem. Commun.* **1986**, 459–460. (c) Pill, T.; Beck, W. Z. *Naturforsch. B* **1993**, *48*, 1461–1469. (d) Zhou, Y.; Wagner, B.; Polborn, K.; Sünkel, K.; Beck, W. Z. *Naturforsch. B* **1994**, *49*, 1193–1202. (e) Kuduk-Jaworska, J. *Transition Met. Chem. (London)* **1994**, *19*, 296–298. (f) RajanBabu, T. V.; Ayers, T. A. *Tetrahedron Lett.* **1994**, *35*, 4295–4298. (g) Appelt, A.; Willis, A. C.; Wild, S. B. *J. Chem. Soc., Chem. Commun.* **1988**, 938–940. (h) Andrews, M. A.; Gould, G. L. *Organometallics* **1991**, *10*, 387–389. (i) Andrews, M. A.; Voss, E. J.; Gould, G. L.; Klooster, W. T.; Koetzle, T. F. *J. Am. Chem. Soc.* **1994**, *116*, 5730–5740.

(9) Steinborn, D.; Junicke, H.; Bruhn, C. *Angew. Chem.* **1997**, *109*, 2803–2805; *Angew. Chem., Int. Ed. Engl.* **1997**, *36*, 2686–2688.

(10) Junicke, H.; Bruhn, C.; Ströhl, D.; Kluge, R.; Steinborn, D. *Inorg. Chem.* **1998**, *37*, 4603–4606.

Wittenberg using solvent signals (¹H, ¹³C) as internal references and Na₂[PtCl₆] (δ(¹⁹⁵Pt) = +4520 ppm) as an external reference. Mass spectra were obtained on an ESI-mass spectrometer LCQ (Finnigan Mat) using ca. 10^{−3} M solutions of the complexes in dry acetone under the following conditions: flow 8 μL/min, ESI spray voltage 4.1 kV; capillary temperature 200 °C; sheath gas N₂; capillary voltage 34 kV. Microanalyses were performed by the Microanalytical Laboratory in the Chemistry Department at Martin-Luther-Universität Halle-Wittenberg. Hexachloroplatinic acid (Degussa, Saxonia) and all carbohydrates (Aldrich, Merck, Fluka) were obtained commercially, and [(PtMe₃)₄] was prepared as described previously.¹¹ ¹³C-labeled monosaccharides were provided by Omicron Biochemicals, Inc., South Bend, IN. All procedures were performed under anaerobic conditions using Schlenk techniques with purified argon. Acetone was dried over B₂O₃ and distilled under argon.

Synthesis of ¹³C-Labeled 1,2-*O*-Isopropylidene- α -D-glucofuranoses. Singly ¹³C-labeled D-glucoses (C1–C6) were converted to the corresponding ¹³C-labeled 1,2,5,6-di-*O*-isopropylidene- α -D-glucofuranoses according to literature procedures.¹² After recrystallization, the 5,6-*O*-isopropylidene group was removed selectively with sulfuric acid in methanol,¹² yielding ¹³C-labeled 1,2-*O*-isopropylidene- α -D-glucofuranoses. NMR spectra of the free and complexed sugar were obtained on a 600 MHz Varian UNITY Plus spectrometer equipped with a Nalorac 3 mm probe to facilitate the measurement of ¹³C–¹³C coupling constants and enhance spectral S/N ratios of the natural abundance carbon signals.

Synthesis of [PtMe₃(Me₂CO)₃]BF₄ (1). [(PtMe₃)₄] (230 mg, 0.14 mmol) was added to a stirred solution of AgBF₄ (100 mg, 0.51 mmol) in acetone (20 mL) in the dark. After 30 min, AgI was removed by filtration, leaving a colorless solution which was used without further purification.

Synthesis of [PtMe₃L]BF₄. To a solution of **1** (270 mg, 0.51 mmol) in acetone (20 mL) was added with stirring a solution of the carbohydrate L' (0.54 mmol) in acetone (5 mL). After 12 h, the solvent was removed *in vacuo* and the white residue was resolved in dry methylene chloride (10 mL). **Method A:** After 1 h, the white [PtMe₃L]BF₄ precipitate was collected by filtration, washed with a small amount of methylene chloride, and dried under argon. **Method B:** After the addition of hexane (5 mL), the white [PtMe₃L]BF₄ precipitate was collected by filtration, washed with diethyl ether (2 mL), and dried under argon.

Compound 14E (L = 1,2-*O*-Isopropylidene- α -D-glucofuranose, L' = 1,2,5,6-Di-*O*-isopropylidene- α -D-glucofuranose (1A)). **Workup Method A.** Yield: 116 mg (39%). Mp: 60 °C, dec above 145 °C (under argon). Found: C, 26.11; H, 4.93. C₁₂H₂₅BF₄O₆Pt requires C, 26.34; H, 4.61. ¹H NMR (500 MHz, −50 °C, (CD₃)₂CO): δ = 1.03 (s + d, ²J(Pt,H) = 78.8 Hz, 9H, PtCH₃), 6.83 (s, 3H, OH) ppm. ¹H NMR (500 MHz, (CD₃)₂CO): δ = 1.25 (s, 3H, CCH₃), 1.26 (s + d, br, ²J(Pt,H), 9H, PtCH₃), 1.39 (s, 3H, CCH₃), 3.88 (dd, 1H, H7, 6.2/8.3 Hz), 3.95 (dd, 1H, H4, 2.6/7.5 Hz), 4.10 (d, 1H, H3, 2.6 Hz), 4.26 (ddd, 1H, H5, 5.7/6.2/7.5 Hz), 4.43 (d, 1H, H2, 3.6 Hz), 5.84 (d, 1H, H1, 3.6 Hz) ppm. ¹³C{¹H} NMR (100 MHz, (CD₃)₂CO): δ = −11.58 (PtCH₃), 26.4 (CH₃), 27.2 (CH₃), 67.6 (C6), 73.7 (C5), 75.2 (C3), 82.5 (C4), 86.6 (C2), 106.2 (C1), 112.7 (OCO) ppm. ¹⁹⁵Pt{¹H} NMR (107 MHz, (CD₃)₂CO): δ = 2350 ppm. MS: *m/z* (obsd/calcd, %) 457 (2/2), 459 (77/86), 460 (100/100), 461 (73/80), 462 (10/11), 463 (20/20), 464 (4/3).

Compound 14E*. (All ¹³C-labeled compounds are marked with an asterisk.) ¹³C{¹H} NMR (150 MHz, (CD₃)₂CO): ¹J_{C₆,C₅} = 34.4 Hz, ¹J_{C₅,C₄} = 48.7 Hz, ¹J_{C₄,C₃} = 38.3 Hz, ²J_{C₆,C₄} = 0 Hz, ²J_{C₅,C₃} = 0.8 Hz, ³J_{C₆,C₃} = 1.7 Hz, ³J_{C₄,H₆} = 3.1 Hz, ³J_{C₃,H₅} = 2.0 Hz, ³J_{C₆,H₄} = 0 Hz.

Compound 15E (L = 3-*O*-Acetyl-1,2-*O*-isopropylidene- α -D-glucofuranose, L' = 3-*O*-Acetyl-1,2,5,6-di-*O*-isopropylidene- α -D-glucofuranose (2A)). **Workup Method B.** Yield: 168 mg (52%). Mp: 133 °C, dec above 142 °C (under argon). Found: C, 28.15; H, 4.25. C₁₄H₂₇BF₄O₇Pt requires C, 28.53; H, 4.62. ¹H NMR (500 MHz, −50 °C, (CD₃)₂CO): δ = 1.04/1.10/1.22 (s + d, ²J(Pt,H) = 78.8/78.2/80.4 Hz, 9H, PtCH₃), 6.65 (s, 1H, OH), 6.82 (s, 1H, OH) ppm. ¹H NMR

(11) Baldwin, J. C.; Kaska, W. C. *Inorg. Chem.* **1975**, *14*, 2020.

(12) Schmidt, O. T. *Methods Carbohydr. Chem.* **1963**, *2*, 318–325.

(500 MHz, $(\text{CD}_3)_2\text{CO}$): $\delta = 1.25$ (s + d, br, $^2J(\text{Pt},\text{H}) = 79.3$ Hz, 9H, PtCH_3), 1.26 (s, 3H, Me), 1.43 (s, 3H, Me), 2.04 (s, 3H, $\text{Me}_{(\text{acc})}$), 3.91 (dd, 1H, H_7 , 5.1/8.3 Hz), 4.04 (dd, 1H, H_6 , 5.8/8.3 Hz), 4.19 (dd, 1H, H_4 , 2.9/7.3 Hz), 4.23 (ddd, 1H, H_5 , 5.1/5.8/7.4 Hz), 4.56 (d, 1H, H_2 , 3.7 Hz), 5.14 (d, 1H, H_3 , 2.9 Hz), 5.89 (d, 1H, H_1 , 3.7 Hz) ppm. $^{13}\text{C}\{^1\text{H}\}$ NMR (100 MHz, $(\text{CD}_3)_2\text{CO}$): $\delta = -12.1$ (s + d, br, PtCH_3), 20.6 ($\text{CH}_3_{(\text{acc})}$), 26.3 (CH_3), 26.9 (CH_3), 67.4 (C6), 73.4 (C5), 76.8 (C3), 83.9 (C4), 84.2 (C2), 106.2 (C1), 112.5 (OCO), 170.2 ($\text{CO}_{(\text{acc})}$) ppm. $^{195}\text{Pt}\{^1\text{H}\}$ NMR (107 MHz, $(\text{CD}_3)_2\text{CO}$): $\delta = 2624$ ppm. MS: m/z (obsd/calcd, %) 499 (2/2), 501 (88/84), 502 (100/100), 503 (74/81), 504 (14/13), 505 (21/20), 506 (3/3).

Compound 16E (L = 3-O-(Methylsulfonyl)-1,2-O-isopropylidene- α -D-glucofuranose, L' = 3-O-(Methylsulfonyl)-1,2;5,6-di-O-isopropylidene- α -D-glucofuranose (3A)). Workup Method B. Yield: 143 mg (42%). Mp: 125 °C, dec above 130 °C (under argon). Found: C, 24.38; H, 4.78. $\text{C}_{13}\text{H}_{27}\text{BF}_4\text{O}_7\text{Pt}$ requires C, 24.97; H, 4.35. ^1H NMR (500 MHz, $-\text{50}^\circ\text{C}$, $(\text{CD}_3)_2\text{CO}$): $\delta = 1.02/1.08/1.21$ (s + d, $^2J(\text{Pt},\text{H}) = 78.9/78.4/79.9$ Hz, 9H, PtCH_3), 6.63 (s, 1H, OH), 6.80 (s, 1H, OH) ppm. ^1H NMR (500 MHz, $(\text{CD}_3)_2\text{CO}$): $\delta = 1.25$ (s + d, br, $^2J(\text{Pt},\text{H}) = 79.3$ Hz, 9H, PtCH_3), 1.26 (s, 3H, Me), 1.43 (s, 3H, Me), 2.04 (s, 3H, Me), 3.89 (dd, 1H, H_7 , 4.9/8.4 Hz), 4.10 (dd, 1H, H_6 , 6.1/8.4 Hz), 4.16 (dd, 1H, H_4 , 2.7/7.9 Hz), 4.24 (ddd, 1H, H_5 , 4.8/6.1/7.9 Hz), 4.79 (d, 1H, H_2 , 3.7 Hz), 4.96 (d, 1H, H_3 , 2.9 Hz), 5.98 (d, 1H, H_1 , 3.7 Hz) ppm. $^{13}\text{C}\{^1\text{H}\}$ NMR (100 MHz, $(\text{CD}_3)_2\text{CO}$): $\delta = -12.0$ (s + d, br, PtCH_3), 26.3 (CH_3), 26.9 (CH_3), 38.3 ($\text{CH}_3\text{-S}$), 67.9 (C6), 73.1 (C5), 80.8 (C3), 83.5 (C4), 84.8 (C2), 106.2 (C1), 113.0 (OCO) ppm. $^{195}\text{Pt}\{^1\text{H}\}$ NMR (107 MHz, $(\text{CD}_3)_2\text{CO}$): $\delta = 2618$ ppm. MS: m/z (obsd/calcd, %) 535 (2/2), 537 (85/84), 538 (100/100), 539 (86/85), 540 (24/18), 541 (20/24), 542 (3/4).

Compound 17E (L = 1,2-O-Isopropylidene- α -D-allofuranose, L' = 1,2;5,6-Di-O-isopropylidene- α -D-allofuranose (4A)). Workup Method A. Yield: 128 mg (42%). Mp: 85 °C, dec above 155 °C (under argon). Found: C, 26.52; H, 4.43. $\text{C}_{12}\text{H}_{25}\text{BF}_4\text{O}_6\text{Pt}$ requires C, 26.34; H, 4.61. ^1H NMR (500 MHz, $-\text{50}^\circ\text{C}$, $(\text{CD}_3)_2\text{CO}$): $\delta = 1.03/1.09$ (s + d, $^2J(\text{Pt},\text{H}) = 78.8/78.3$ Hz, 9H, PtCH_3), 6.65 (s, 2H, OH), 6.82 (s, 1H, OH) ppm. ^1H NMR (500 MHz, $(\text{CD}_3)_2\text{CO}$): $\delta = 1.22$ (s, br, 9H, PtCH_3), 1.22 (s, 3H, CCH_3), 1.35 (s, 3H, CCH_3), 3.81 (dd, 1H, H_7 , 5.3/8.7 Hz), 3.88 (dd, 1H, H_4 , 9.2/3.5 Hz), 4.02 (dd, 1H, H_6 , 6.4/8.7 Hz), 4.12 (ddd, 1H, H_5 , 5.2/6.2/9.2 Hz), 4.55 (dd, 1H, H_2 , 3.9/5.9 Hz), 4.78 (d, 1H, H_3 , 5.9 Hz), 5.26 (d, 1H, H_1 , 3.9 Hz) ppm. $^{13}\text{C}\{^1\text{H}\}$ NMR (100 MHz, $(\text{CD}_3)_2\text{CO}$): $\delta = -11.40$ (s + d, $^1J(\text{Pt},\text{C}) = 814$ Hz, Pt-CH_3), 26.6 (CH_3), 26.9 (CH_3), 67.8 (C6), 76.8 (C3), 83.2 (C5), 87.2 (C2), 88.5 (C4), 103.7 (C1), 110.9 (OCO) ppm. $^{195}\text{Pt}\{^1\text{H}\}$ NMR (107 MHz, $(\text{CD}_3)_2\text{CO}$): $\delta = 2520$ ppm. MS: m/z (obsd/calcd, %) 457 (3/2), 459 (65/86), 460 (100/100), 461 (80/80), 462 (30/11), 463 (15/20), 464 (9/3).

Compound 18E (L = 1,2-O-Isopropylidene-2-keto-L-gulonic Acid, L' = 1,2;4,6-Di-O-isopropylidene-2-keto-L-gulonic Acid (5A)). Workup Method A. Yield: 200 mg (65%). Mp: 102 °C under dec (under argon). Found: C, 26.25; H, 4.52. $\text{C}_{12}\text{H}_{23}\text{BF}_4\text{O}_7\text{Pt}$ requires C, 25.67; H, 4.10. ^1H NMR (500 MHz, $-\text{50}^\circ\text{C}$, $(\text{CD}_3)_2\text{CO}$): $\delta = 1.03/1.27$ (s + d, $^2J(\text{Pt},\text{H}) = 78.3/79.9$ Hz, 9H, PtCH_3), 6.75 (s, 1H, OH), 6.85 (s, 1H, OH), 12.1 (s, 1H, $b_{1/2} = 34$ Hz, COOH) ppm. ^1H NMR (500 MHz, $(\text{CD}_3)_2\text{CO}$): $\delta = 1.23$ (s + d, br, $^2J(\text{Pt},\text{H}) = 79.3$ Hz, 9H, PtCH_3), 1.39 (s, 3H, Me), 1.46 (s, 3H, Me), 3.94 (d, 1H, H_5 , 13.6 Hz), 4.16 (m, 2H, H_3/H_4), 4.39 (s, 1H, H_2), 4.69 (s, 1H, H_1) ppm. $^{13}\text{C}\{^1\text{H}\}$ NMR (100 MHz, $(\text{CD}_3)_2\text{CO}$): $\delta = -12.0$ (s + d, br, PtCH_3), 25.9 (CH_3), 27.2 (CH_3), 60.4 (C5), 73.5 (C3), 75.1 (C4), 82.9 (C2), 109.8 (C1), 114.9 (C_i), 168.1 (C_{OoH}) ppm. $^{195}\text{Pt}\{^1\text{H}\}$ NMR (107 MHz, $(\text{CD}_3)_2\text{CO}$): $\delta = 2541$ ppm. MS: m/z (obsd/calcd, %) no peak found.

Compound 19E (L = 2,3-Di-O-isopropylidene- α -L-sorbofuranose, L' = 2,3;4,6-Di-O-isopropylidene- α -L-sorbofuranose (6A)). Workup Method A. Reaction time: 48 h. Yield: 205 mg (69%). Mp: 90 °C, dec above 138 °C (under argon). Found: C, 26.56; H, 4.81. $\text{C}_{12}\text{H}_{25}\text{BF}_4\text{O}_6\text{Pt}$ requires C, 26.35; H, 4.60. ^1H NMR (500 MHz, $-\text{50}^\circ\text{C}$, $(\text{CD}_3)_2\text{CO}$): $\delta = 1.04/1.10$ (s + d, $^2J(\text{Pt},\text{H}) = 78.9/78.3$ Hz, 9H, PtCH_3), 6.66 (s, 2H, OH), 6.85 (s, 1H, OH) ppm. ^1H NMR (500 MHz, $(\text{CD}_3)_2\text{CO}$): $\delta = 1.18$ (s + d, br, $^2J(\text{Pt},\text{H}) = 79.3$ Hz, 9H, PtCH_3), 1.32 (s, 3H, Me), 1.40 (s, 3H, Me), 3.67 (m, 2H, H_1/H_2), 3.84 (d, 1H, H_7 , 13.4 Hz), 4.04 (dd, 1H, H_5 , 2.3/3.48 Hz), 4.10 (dd, 1H, H_6 , 2.3/13.3 Hz), 4.31 (d, 1H, H_4 , 2.2 Hz), 4.38 (s, 1H, H_3) ppm. $^{13}\text{C}\{^1\text{H}\}$ NMR

(100 MHz, $(\text{CD}_3)_2\text{CO}$): $\delta = -11.8$ (s + d, br, PtCH_3), 27.1 (CH_3), 27.9 (CH_3), 60.9 (C6), 63.4 (C1, $b_{1/2} = 9.0$ Hz), 73.3 (C3), 74.1 (C4), 85.1 (C2), 97.9 (C1), 112.3 (C_i) ppm. $^{195}\text{Pt}\{^1\text{H}\}$ NMR (107 MHz, $\text{CD}_2\text{-Cl}_2$): $\delta = 2560$ ppm. MS: m/z (obsd/calcd, %) 457 (5/2), 459 (86/86), 460 (100/100), 461 (75/80), 462 (10/11), 463 (18/20), 464 (3/3).

Compound 20E (L = 1,2-O-Isopropylidene- α -D-xylofuranose (12B), L = L'). Workup Method B. Yield: 120 mg (43%). Mp: 89 °C under dec (under argon). Found: C, 26.11; H, 5.29. $\text{C}_{11}\text{H}_{23}\text{BF}_4\text{O}_5\text{-Pt}$ requires C, 25.60; H, 5.65. ^1H NMR (500 MHz, $-\text{50}^\circ\text{C}$, $(\text{CD}_3)_2\text{-CO}$): $\delta = 1.04/1.10/1.22$ (s + d, $^2J(\text{Pt},\text{H}) = 78.9/78.5/80.0$ Hz, 9H, PtCH_3), 6.64 (s, 1H, OH), 6.80 (s, 1H, OH) ppm. ^1H NMR (500 MHz, $(\text{CD}_3)_2\text{CO}$): $\delta = 1.27$ (s + d, br, $^2J(\text{Pt},\text{H}) = 79.8$ Hz, 9H, PtCH_3), 1.27 (s, 3H, Me), 1.40 (s, 3H, Me), 3.87 (d, 1H, H_6 , 13.7 Hz), 3.95 (dt, 1H, H_4 , 0.9/2.4 Hz), 4.13 (dd, 1H, H_5 , 2.3/13.5 Hz), 4.27 (d, 1H, H_3 , 2.1 Hz), 4.47 (d, 1H, H_2 , 3.8 Hz), 5.86 (d, 1H, H_1 , 3.6 Hz) ppm. $^{13}\text{C}\{^1\text{H}\}$ NMR (100 MHz, $(\text{CD}_3)_2\text{CO}$): $\delta = -12.1$ (s + d, br, PtCH_3), 26.4 (CH_3), 27.0 (CH_3), 60.7 (C6), 72.5 (C3), 74.0 (C4), 85.7 (C2), 106.2 (C1), 111.9 (C_i) ppm. $^{195}\text{Pt}\{^1\text{H}\}$ NMR (107 MHz, (CD_2Cl_2)): $\delta = 2627$ ppm. MS: m/z (obsd/calcd, %) 427 (6/2), 429 (85/86), 430 (100/100), 431 (73/80), 432 (10/11), 433 (20/20), 434 (3/3).

Compound 21E (L = 5,6-O-Isopropylidene-D-gulonon- γ -lactone (13B), L = L'). Workup Method B. Yield: 156 mg (52%). Mp: 112 °C, dec above 131 °C (under argon). Found: C, 26.21; H, 4.86. $\text{C}_{12}\text{H}_{23}\text{-BF}_4\text{O}_6\text{Pt}$ requires C, 26.44; H, 4.25. ^1H NMR (500 MHz, $-\text{50}^\circ\text{C}$, $(\text{CD}_3)_2\text{CO}$): $\delta = 1.04/1.11/1.23$ (s + d, $^2J(\text{Pt},\text{H}) = 78.6/78.6/79.6$ Hz, 9H, PtCH_3), 6.66 (s, 2H, OH), 6.77 (s, 2H, OH) ppm. ^1H NMR (500 MHz, $(\text{CD}_3)_2\text{CO}$): $\delta = 1.27$ (s + d, br, $^2J(\text{Pt},\text{H}) = 78.5$ Hz, 9H, PtCH_3), 1.32 (s, 3H, Me), 1.37 (s, 3H, Me), 3.88 (dd, 1H, H_6 , 6.6/8.5 Hz), 4.14 (dd, 1H, H_5 , 6.8/8.5 Hz), 4.33 (dq, 1H, H_4 , 6.8/8.5 Hz), 4.58 (dd, 1H, H_3 , 3.7/8.5 Hz), 4.98 (d, 1H, H_1 , 5.6 Hz), 5.01 (dd, 1H, H_2 , 3.6/5.0 Hz) ppm. $^{13}\text{C}\{^1\text{H}\}$ NMR (100 MHz, $(\text{CD}_3)_2\text{CO}$): $\delta = -11.8$ (s + d, br, PtCH_3), 25.8 (CH_3), 26.8 (CH_3), 65.0 (C6), 76.2 (C5), 77.2 (C3), 81.5 (C4), 114.7 (C2), 174.0 (C1) ppm. $^{195}\text{Pt}\{^1\text{H}\}$ NMR (107 MHz, $(\text{CD}_3)_2\text{CO}$): $\delta = 2630$ ppm. MS: m/z (obsd/calcd, %) 455 (3/2), 457 (78/86), 458 (100/100), 459 (82/80), 460 (10/11), 461 (15/20), 462 (15/3).

Compound 22D (L = 2,3;4,6-Di-O-isopropylidene- α -L-sorbofuranose (6A)). Workup Method B. Reaction time: 5 h. Yield: 145 mg (45%). Mp: 83 °C, dec above 132 °C (under argon). Found: C, 31.56; H, 5.18. $\text{C}_{15}\text{H}_{29}\text{BF}_4\text{O}_6\text{Pt}$ requires C, 30.69; H, 4.98. ^1H NMR (500 MHz, $-\text{50}^\circ\text{C}$, $(\text{CD}_3)_2\text{CO}$): $\delta = 1.04/1.11/1.28$ (s + d, $^2J(\text{Pt},\text{H}) = 78.8/78.1/80.4$ Hz, 9H, PtCH_3), 6.77 (s, 1H, OH) ppm. ^1H NMR (500 MHz, $(\text{CD}_3)_2\text{CO}$): $\delta = 1.25$ (s, 3H, Me), 1.28 (s + d, br, $^2J(\text{Pt},\text{H}) = 74.7$ Hz, 9H, PtCH_3), 1.33 (s, 3H, Me), 1.41 (s, 3H, Me), 1.42 (s, 3H, Me), 3.67 (m, 2H, H_1/H_2), 3.83 (d, 1H, H_7 , 13.3 Hz), 4.04 (dd, 1H, H_5 , 2.3/2.4 Hz), 4.10 (dd, 1H, H_6 , 2.3/13.3 Hz), 4.32 (d, 1H, H_4 , 2.3 Hz), 4.38 (s, 1H, H_3) ppm. $^{13}\text{C}\{^1\text{H}\}$ NMR (100 MHz, $(\text{CD}_3)_2\text{CO}$): $\delta = -11.8$ (s + d, br, PtCH_3), 19.0 (CH_3), 27.1 (CH_3), 27.8 (CH_3), 29.3 (CH_3), 60.9 (C6), 63.4 (C1, $b_{1/2} = 8.5$ Hz), 73.1 (C3), 74.2 (C4), 85.2 (C5), 97.9 (C2), 112.3 (C_i), 115.8 (C_i) ppm. $^{195}\text{Pt}\{^1\text{H}\}$ NMR (107 MHz, CD_2Cl_2): $\delta = 2642$ ppm. MS: m/z (obsd/calcd, %) 497 (3/2), 499 (88/83), 500 (100/100), 501 (78/81), 502 (13/14), 503 (23/20), 504 (4/3).

Compound 23D (L = 1,2;3,4-Di-O-isopropylidene- α -D-galactopyranose (7A)). Workup Method B. Yield: 153 mg (48%). Mp: 82 °C, dec above 112 °C (under argon). Found: C, 31.30; H, 5.23. $\text{C}_{15}\text{H}_{29}\text{-BF}_4\text{O}_6\text{Pt}$ requires C, 30.69; H, 4.98. ^1H NMR (500 MHz, $-\text{50}^\circ\text{C}$, $(\text{CD}_3)_2\text{CO}$): $\delta = 1.10/1.21/1.27$ (s + d, $^2J(\text{Pt},\text{H}) = 79.1/80.6/81.2$ Hz, 9H, PtCH_3), 6.78 (s, 1H, OH) ppm. ^1H NMR (500 MHz, $(\text{CD}_3)_2\text{CO}$): $\delta = 1.24$ (s + d, br, $^2J(\text{Pt},\text{H}) = 78.4$ Hz, 9H, PtCH_3), 1.29 (s, 3H, Me), 1.30 (s, 3H, Me), 1.35 (s, 3H, Me), 1.46 (s, 3H, Me), 3.66 (m, 2H, H_6/H_7), 3.83 (m, 1H, H_5), 4.29 (dd, 1H, H_4 , 1.8/8.1 Hz), 4.30 (dd, 1H, H_2 , 2.3/5.0 Hz), 4.59 (dd, 1H, H_3 , 2.3/8.0 Hz), 5.45 (d, 1H, H_1 , 5.1 Hz) ppm. $^{13}\text{C}\{^1\text{H}\}$ NMR (100 MHz, $(\text{CD}_3)_2\text{CO}$): $\delta = -11.6$ (s + d, br, PtCH_3), 24.6 (CH_3), 25.2 (CH_3), 26.3 (CH_3), 26.4 (CH_3), 62.2 (C6, $b_{1/2} = 10.9$ Hz), 69.5 (C4), 71.6 (C3), 71.7 (C4), 71.9 (C2), 97.2 (C1), 108.9 (C_i), 109.5 (C_i, $b_{1/2} = 7.4$ Hz) ppm. $^{195}\text{Pt}\{^1\text{H}\}$ NMR (107 MHz, $(\text{CD}_3)_2\text{CO}$): $\delta = 2658$ ppm. MS: m/z (obsd/calcd, %) 497 (3/2), 499 (75/83), 500 (100/100), 501 (79/81), 502 (12/14), 503 (19/20), 504 (3/3).

Compound 24D (L = 2,3,4,5-Di-*O*-isopropylidene- β -D-fructopyranose (8A)). Workup Method B. Yield: 199 mg (62%). Mp: 74 °C, dec above 98 °C (under argon). Found: C, 31.16; H, 4.73. C₁₅H₂₉BF₄O₆Pt requires C, 30.69; H, 4.98. ¹H NMR (500 MHz, –50 °C, (CD₃)₂CO): δ = 1.10/1.22/1.27 (s + d, ²J(Pt,H) = 78.5/80.9/80.2 Hz, 9H, PtCH₃), 6.77 (s, 1H, OH) ppm. ¹H NMR (500 MHz, (CD₃)₂CO): δ = 1.29 (s, 3H, Me), 1.30 (s + d, br, ²J(Pt,H) = 79.4 Hz, 9H, PtCH₃), 1.36 (s, 6H, Me), 1.46 (s, 3H, Me), 3.56 (m, 3H, H1/H2/H7), 3.85 (dd, 1H, H6, 1.9/12.9 Hz), 4.21 (dd, 1H, H5, 1.3/7.9 Hz), 4.36 (d, 1H, H3, 2.5 Hz), 4.60 (dd, 1H, H4, 2.5/7.8 Hz) ppm. ¹³C{¹H} NMR (100 MHz, (CD₃)₂CO): δ = –11.6 (s + d, br, ²J(Pt,C) = 782 Hz, PtCH₃), 24.4 (CH₃), 25.9 (CH₃), 26.3 (CH₃), 26.9 (CH₃), 61.9 (C6), 64.9 (C1, br, b_{1/2} = 10.8 Hz), 70.9 (C3), 71.3 (C4), 72.0 (C5), 104.5 (C2), 109.0 (C_i), 109.5 (C_i) ppm. ¹⁹⁵Pt{¹H} NMR (107 MHz, (CD₃)₂CO): δ = 2618 ppm. MS: *m/z* (obsd/calcd, %) 497 (2/2), 499 (80/83), 500 (100/100), 501 (80/81), 502 (18/14), 503 (20/20), 504 (2/3).

Synthesis of [PtMe₃L(H₂O)]BF₄ (24D') (L = 2,3,4,5-Di-*O*-isopropylidene- β -D-fructopyranose (8A)). [PtMe₃L]BF₄ (24D) (100 mg, 0.17 mmol) was dissolved in wet methylene chloride. Within 24 h, 24D' precipitated as colorless crystals which were isolated by filtration and dried under argon. Yield: 75 mg (73%). Mp: 98 °C, dec above 124 °C (under argon). Found: C, 29.42; H, 5.34. C₁₅H₃₁BF₄O₇Pt requires C, 29.78; H, 5.17. ¹H NMR (500 MHz, –50 °C, (CD₃)₂CO): δ = 1.04/1.11 (s + d, ²J(Pt,H) = 79.5/79.9 Hz, 9H, PtCH₃), 6.66 (s, 2H, OH₂); 6.86 (s, 1H, OH) ppm. ¹H NMR (500 MHz, (CD₃)₂CO): δ = 1.21 (s + d, br, ²J(Pt,H) = 79.1 Hz, 9H, PtCH₃), 1.29 (s, 3H, Me), 1.36 (s, 6H, Me), 1.46 (s, 3H, Me), 3.56 (m, 3H, H1/H2/H7), 3.85 (dd, 1H, H6, 1.9/12.9 Hz), 4.21 (dd, 1H, H5, 1.3/7.9 Hz), 4.36 (d, 1H, H3, 2.5 Hz), 4.60 (dd, 1H, H4, 2.5/7.8 Hz) ppm. ¹³C{¹H} NMR (100 MHz, (CD₃)₂CO): δ = –11.6 (s + d, br, ²J(Pt,C) = 782 Hz, PtCH₃), 24.4 (CH₃), 25.9 (CH₃), 26.3 (CH₃), 26.9 (CH₃), 61.9 (C6), 64.9 (C1, br, b_{1/2} = 5.0 Hz), 70.9 (C3), 71.3 (C4), 72.0 (C5), 104.5 (C2), 109.0 (C_i), 109.5 (C_i) ppm. ¹⁹⁵Pt{¹H} NMR (107 MHz, (CD₃)₂CO): δ = 2530 ppm. MS: *m/z* (obsd/calcd, %) no peak found.

Synthesis of [PtMe₃L]BF₄ (25D) (L = 1,2:5,6-Di-*O*-isopropylidene- α -D-glucofuranose). [PtMe₃L]BF₄ (14E) (100 mg, 0.18 mmol) was dissolved in acetone, and after 1 week the solvent was removed in vacuo, leaving a solid residue. Extraction with 5 mL of methylene chloride gave a white powder of 25D. Yield: 98 mg (91%). Mp: 70 °C, dec above 127 °C (under argon). Found: C, 30.21; H, 4.64. C₁₅H₂₉BF₄O₆Pt requires C, 30.68; H, 4.97. ¹H NMR (500 MHz, –50 °C, (CD₃)₂CO): δ = 1.03/1.09/1.22 (s + d, ²J(Pt,H) = 79.1/78.0/80.7 Hz, 9H, PtCH₃), 6.91 (s, 1H, OH) ppm. ¹H NMR (500 MHz, (CD₃)₂CO): δ = 1.27 (s + d, br, ²J(Pt,H) = 79.9 Hz, 9H, PtCH₃), 1.27 (s, 3H, Me), 1.28 (s, 3H, Me), 1.34 (s, 3H, Me), 1.41 (s, 3H, Me), 3.85 (dd, 1H, H7, 8.3/5.9 Hz), 3.96 (dd, 1H, H4, 2.9/7.5 Hz) 4.00 (dd, 1H, H6, 6.2/8.3), 4.10 (dd, 1H, H3, 2.7/4.6 Hz), 4.25 (ddd, 1H, H5, 6.2/5.9/7.5 Hz), 4.49 (d, 1H, H2, 3.6 Hz), 5.85 (d, 1H, H1, 3.6 Hz) ppm. ¹³C{¹H} NMR (100 MHz, (CD₃)₂CO): δ = –12.1 (s + d, br, PtCH₃), 25.6 (CH₃), 26.4 (CH₃), 27.0 (CH₃), 27.1 (CH₃), 67.6 (C6), 73.6 (C5), 75.2 (C3), 82.5 (C4), 86.6 (C2), 106.0 (C1), 109.3 (C_i), 112.0 (C_i) ppm. ¹⁹⁵Pt{¹H} NMR (107 MHz, (CD₃)₂CO): δ = 2600 ppm. MS: *m/z* (obsd/calcd, %) 497 (3/2), 499 (82/83), 500 (100/100), 501 (79/81), 502 (14/14), 503 (20/20), 504 (3/3).

X-ray Crystal Structure Determinations. Colorless single crystals of [PtMe₃(C₉H₁₆O₆)]BF₄ (19E) and [PtMe₃(C₁₂H₂₀O₆)(H₂O)]BF₄ (24D') having platelike characteristics were mounted on a glass fiber using perfluorinated ether and analyzed under a stream of cold nitrogen. Data collections was performed with an area detector using graphite-monochromatized MoK α radiation (λ_0 = 0.710 73 Å), and the data sets were corrected numerically for absorption T_{\min}/T_{\max} = 0.46/0.16 for 19E and 0.48/0.33 for 24D' (Table 1). The structures were solved by direct methods (SHELXS-86)¹³ and refined using the full-matrix least-squares method against F^2 (SHELXL-93).¹⁴ All non-hydrogen atoms were refined anisotropically; hydrogen atoms were included in calculated positions and refined with isotropic displacement parameters according to the riding model.

(13) Sheldrick, G. M. *SHELXS-86, Program for the Solution of Crystal Structures*; University of Göttingen, Germany, 1986.

(14) Sheldrick, G. M. *SHELXL-93, Program for the Refinement of Crystal Structures*; University of Göttingen, Germany, 1993.

Table 1. X-ray Diffraction Data for 19E and 24D'

	19E	24D'
formula	C ₁₂ H ₂₅ BF ₄ O ₆ Pt	C ₁₅ H ₃₁ BF ₄ O ₇ Pt
formula weight	547.22	605.30
crystal dimensions (mm)	0.17 × 0.11 × 0.06	0.30 × 0.10 × 0.10
crystal color	colorless	colorless
temperature (K)	200(2)	220(2)
crystal system	monoclinic	orthorhombic
space group	P2 ₁	P2 ₁ 2 ₁ 2 ₁
<i>a</i> (Å)	8.607(3)	9.851(2)
<i>b</i> (Å)	9.955(4)	11.141(4)
<i>c</i> (Å)	11.415(4)	20.418(6)
β (deg)	111.09(4)	
<i>V</i> (Å ³)	912.6(6)	2240.8(11)
<i>Z</i>	2	4
<i>D</i> _{calcd} (g/cm ³)	1.991	1.794
diffractometer	STOE IPDS	STOE IPDS
μ (mm ⁻¹)	7.750	6.325
refinement, <i>wR</i> ² _a	0.1353	0.1280
refinement, <i>R</i> ₁	0.0560	0.0581
goodness of fit on <i>F</i> ²	1.091	0.955
absolute structure parameter	0.02(2)	0.00(2)

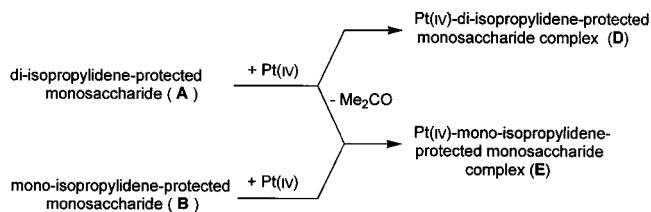
$$^a wR2 = [\sum[w(F_o^2 - F_c^2)^2]/\sum[w(F_o^2)^2]]^{1/2}.$$

Kinetics. [PtMe₃(Me₂CO)₃]BF₄ (1) (270 mg, 0.51 mmol) was prepared as described above, and the solvent was removed *in vacuo*. Compound 1 was dissolved in [D₆]acetone at 27 °C, the diprotected carbohydrate (0.05 mmol) was added, and the ¹H NMR spectra were recorded at 10 min intervals over a period of 16 h on a Varian VRX 500 spectrometer. Rate constants were calculated by integration of the signals of the methyl protons in the protecting group using the Varian VNMR 5.3 software.

Results and Discussion

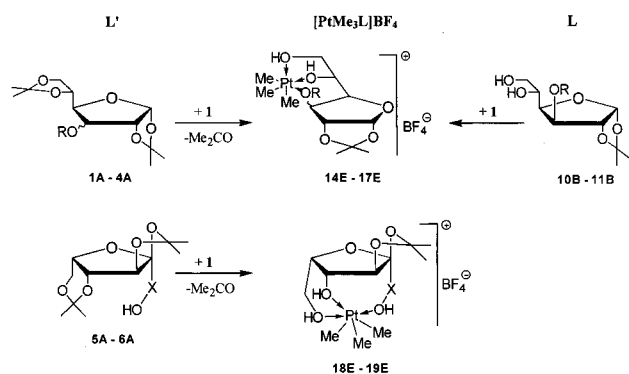
A. Platinum Complexes with Monoprotected Carbohydrate Ligands. 1. Synthesis. The trimethylplatinum(IV) cation reacts with diisopropylidene-protected monosaccharides (A) in anhydrous acetone with or without the loss of an isopropylidene group to give new platinum(IV) complexes with mono (E) or di (D) isopropylidene-protected carbohydrate ligands. Type E complexes can also be obtained directly from the monoprotected carbohydrates (B) (Scheme 2).

Scheme 2



[PtMe₃(Me₂CO)₃]BF₄ (1) reacts in acetone with 1,2:5,6-di-*O*-isopropylidene- α -D-glucofuranose (1A), 3-*O*-acetyl-1,2:5,6-di-*O*-isopropylidene- α -D-glucofuranose (2A), 3-*O*-(methylsulfonyl)-1,2:5,6-di-*O*-isopropylidene- α -D-glucofuranose (3A), 1,2:5,6-di-*O*-isopropylidene- α -D-allofuranose (4A), 2,3:4,6-di-*O*-isopropylidene-2-keto-L-gulonic acid (5A), and 2,3:4,6-di-*O*-isopropylidene- α -L-sorbofuranose (6A) to give trimethyl-(carbohydrate)platinum tetrafluoroborate complexes 14E–19E in moderate to good yields (Scheme 3). Platinum complexation is accompanied by the cleavage of one isopropylidene group, and the platinum coordinates to the liberated hydroxyl groups and to a third hydroxyl group or oxygen donor if functionalized monosaccharides are used. As shown by the preparation of complexes 14E and 15E, 1,2-*O*-isopropylidene- α -D-glucofuranose (10B) and 3-*O*-acetyl-1,2-*O*-isopropylidene- α -D-glucofuranose (11B) can also be used as starting materials. In these

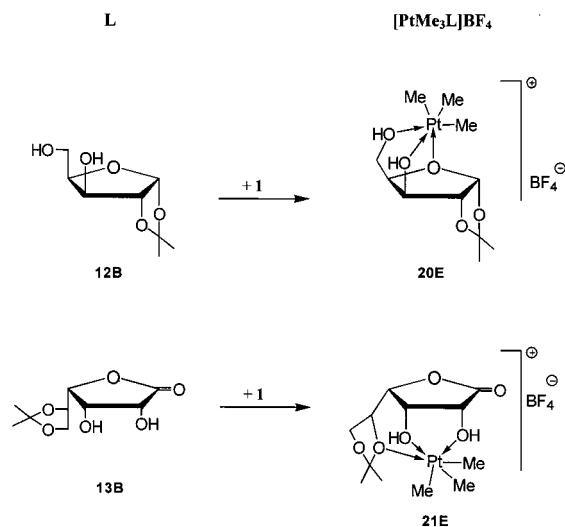
Scheme 3



L'	R	X	$[\text{PtMe}_3\text{L}]\text{BF}_4$ (Yield)	L
1A	H ^a		14E (39%)	1,2- <i>O</i> -isopropylidene- α -D-glucofuranose
2A	COMe		15E (52%)	3- <i>O</i> -acetyl-1,2- <i>O</i> -isopropylidene- α -D-glucofuranose
3A	SO ₂ Me		16E (42%)	3- <i>O</i> -methylsulfonyl-1,2- <i>O</i> -isopropylidene- α -D-glucofuranose
4A	H ^b		17E (42%)	1,2- <i>O</i> -isopropylidene- α -D-allofuranose
5A		CO	18E (65%)	2,3- <i>O</i> -isopropylidene-2-keto-L-gulonic acid
6A		CH ₂	19E (69%)	2,3- <i>O</i> -isopropylidene- α -L-sorbofuranose
10B ^c	H		14E (82%)	1,2- <i>O</i> -isopropylidene- α -D-glucofuranose
11B ^c	COMe		15E (52%)	3- <i>O</i> -acetyl-1,2- <i>O</i> -isopropylidene- α -D-glucofuranose

^a OH_{above} the ring; ^b OH_{beneath} the ring; ^c ligand L.

Scheme 4



L	$[\text{PtMe}_3\text{L}]\text{BF}_4$ (Yield)	L
12B	20E (43%)	1,2- <i>O</i> -isopropylidene- α -D-xylofuranose
13B	21E (52%)	5,6- <i>O</i> -isopropylidene-D-gulono-1,4-lactone

cases, complex formation proceeds without the loss of a protecting group (Scheme 3).

1,2-*O*-Isopropylidene- α -D-xylofuranose (**12B**; protecting group anti to OH) and 5,6-*O*-isopropylidene-L-gulono-1,4-lactone (**13B**; protecting group syn to OH) react in the same way to give complexes $[\text{PtMe}_3\text{L}]\text{BF}_4$ (**20E**, L = **12B**; **21E**, L = **13B**) without the loss of a protecting group (Scheme 4). In both complexes the carbohydrate ligand coordinates via its two OH groups, these presumably being the strongest donor sites. The facial coordination mode is completed by the ring oxygen of the furanose (**20E**) or of the isopropylidene group (**21E**).

The platinum-carbohydrate complexes **14E–21E** were isolated as white, air- and moisture-sensitive powders or colorless crystals in moderate to good yields (39–82%), and their identities were confirmed by microanalysis, ¹H, ¹³C, and ¹⁹⁵Pt NMR spectroscopy, single-crystal structure analysis (**14E**, ⁹ **19E**), and ESI mass spectroscopy.

During the complex formation (Scheme 3), one of the two isopropylidene groups is lost as acetone, presumably due to the presence of trace amounts of water in the reaction mixture. Adding water to the reaction mixture prevented the formation of **14E**; instead, $[\text{PtMe}_3(\text{H}_2\text{O})_3]\text{BF}_4$ was formed immediately from cleavage of the carbohydrate and acetone ligands. No further cleavage of an isopropylidene group was observed, demonstrating that elimination of the protecting group is platinum-promoted.

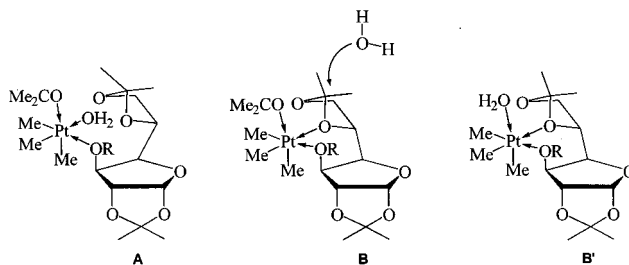
The rate constants were determined for the reaction of **1** with **1A–4A** and **6A** in $[\text{D}_6]$ acetone by NMR spectroscopy, assuming that the reactions are pseudo-first-order. The relative rates are

$$1\text{A}(1.0) > 6\text{A}(0.8) > 4\text{A}(0.7) > 3\text{A}(0.2) > 2\text{A}(0.1) \quad (k \text{ relative to } 1\text{A})$$

$$17.4 \quad 14.2 \quad 11.3 \quad 3.6 \quad 1.8 \quad (\text{absolute } k \text{ in } 10^6 \text{ s}^{-1})$$

These hydrolysis reactions probably proceed via an initial monodentate coordination of the ligand L' through the functional group at C3. Hydrolysis is facilitated by the coordination of water (the resulting acidity of water is estimated to increase by as much as 13 orders of magnitude),¹⁵ which positions the proton donor near the ketal oxygen of the protecting group (intermediate **A**, Scheme 5). Alternatively, an additional coordination of L' through the ketal oxygen of the protecting group (intermediate **B**, Scheme 5) could occur, resulting in enhanced electrophilicity of the ketal carbon. In the latter, the hydrolysis reaction may be facilitated by the enhanced acidity of an aqua ligand (intermediate **B'**, Scheme 5).

Scheme 5



The importance of the precoordination of L' through the functional group at C3 can be derived from the order of the reactivity. The carbohydrate ligands with the weakest donor groups on C3 (COMe (**2A**) and SO₂Me (**3A**)) react more slowly than those with the stronger donating hydroxyl groups (**1A**, **4A**, **6A**). The difference between **1A** and **4A** can be attributed to greater ring strain in the intermediates or transition states of **4A** due to the anti position of the OH group at C3 and the exocyclic isopropylidene group, which will be cleaved off.

2. NMR Spectroscopy. Selected NMR data are shown in Table 2. In ¹H NMR spectra acquired at ambient temperature, the methyl ligands exhibit a broad signal at 1.23–1.27 ppm flanked by platinum satellites. Thus, the donor strength of the carbohydrate can be measured by the chemical shift of the trans-oriented methyl ligands,¹⁶ whose signals lie between the acetone and water ligand signals: $\text{Me}_2\text{CO} < \text{carbohydrate} < \text{H}_2\text{O}$ (for comparison, $[\text{PtMe}_3\text{L}_3]\text{BF}_4$ (L = Me_2CO) $\delta = 1.37$ ppm, (L =

(15) van Eldik, R. *Adv. Inorg. Bioinorg. Mech.* **1984**, *3*, 275–309.

(16) Schlecht, S.; Magull, J.; Fenske, D.; Dehnicke, K. *Angew. Chem.* **1997**, *109*, 2087–2090; *Angew. Chem., Int. Ed. Engl.* **1997**, *36*, 1994–1995.

Table 2. ^1H Chemical Shifts^a of the Methyl Ligands and the Coordinated Hydroxyl/Carboxylic Acid Protons and ^{195}Pt Chemical Shifts for the Complexes **14E–21E**

compd	coord mode	$\delta(^1\text{H})$ [$^2J(\text{Pt,H})$] ^b			δ (^{195}Pt)
		CH_3 (rt)	CH_3 (-50°C)	OH (-50°C)	
14E	OH, OH, OH	1.26 [br]	1.03 [78.8] (9H)	6.83 (3H)	2350
15E	OH, OH, O_{COMe}	1.25 [79.3]	1.04 [78.8] (3H)	6.65 (1H)	2624
			1.10 [78.2] (3H)	6.82 (1H)	
			1.22 [80.4] (3H)		
16E	OH, OH, $\text{O}_{\text{SO}_2\text{Me}}$	1.25 [br]	1.02 [78.9] (3H)	6.63 (1H)	2618
			1.08 [78.4] (3H)	6.80 (1H)	
			1.21 [79.9] (3H)		
17E	OH, OH, OH	1.22 [br]	1.03 [78.8] (6H)	6.65 (2H)	2520
18E	OH, OH, COOH	1.18 [79.3]	1.03 [78.3] (6H)	6.82 (1H)	2541
			1.27 [79.3] (3H)	6.81 (1H)	
				12.1 (1H)	
19E	OH, OH, OH	1.26 [79.3]	1.03 [78.9] (6H)	6.66 (2H)	2560
			1.10 [78.4] (3H)	6.85 (1H)	
			1.04 [78.9] (3H)	6.64 (1H)	
20E	OH, OH, O_{ring}^c	1.27 [79.8]	1.04 [78.9] (3H)	6.64 (1H)	2627
			1.10 [78.5] (3H)	6.80 (1H)	
			1.22 [80.0] (3H)		
21E	OH, OH, $\text{O}_{\text{acetal}}^d$	1.27 [78.5]	1.04 [78.6] (3H)	6.66 (1H)	2630
			1.11 [78.6] (3H)	6.77 (1H)	
			1.23 [79.6] (3H)		

^a In parts per million, in $[\text{D}_6]\text{acetone}$. ^b $^2J_{\text{Pt,H}}$ values in brackets, in hertz; br denotes broadened signal. ^c O_{ring} = furanose ring oxygen. ^d O_{acetal} = acetal oxygen of the isopropylidene group.

H_2O) $\delta = 1.06$ ppm). At -50°C , the broad methyl group signal is split into three sharp signals flanked by platinum satellites, revealing the nonequivalence of the methyl groups. In the complexes **14E** and **17E–19E**, the three and two methyl groups, respectively, have identical chemical shifts by chance. Methyl ligands trans to hydroxyl groups resonate at higher field (1.03–1.10 ppm) compared to those trans to weaker ligands such as the acetal oxygen in **15E–16E** and **20E–21E** (1.21–1.27 ppm). The low-field signal at 1.27 ppm in **18E** indicates that the carboxyl group is a weaker donor compared to the other two hydroxyl groups in the carbohydrate.

The protons of the hydroxyl groups coordinated to the platinum show a broad low-intensity signal at ambient temperature, whereas at -50°C , sharp signals with the expected intensities are observed. Interestingly, in the complexes the hydroxyl protons show no vicinal couplings to carbon-bound hydrogens, but these couplings are observed in the uncomplexed monosaccharides ($^3J_{\text{HOCH}} = 3\text{--}6$ Hz). This difference might be due to an enhanced exchange with solvent due to the higher acidity of the platinum-bound OH groups and/or to changes in the conformation in the C–O torsion angle(s) upon complexation. Because of the low solubility of the noncoordinated monosaccharides in acetone, the different chemical shifts of the hydroxyl protons in the coordinated and noncoordinated carbohydrates could be determined only for **14E**, **18E**, and **19E**. In these cases, platinum coordination induces a downfield shift of 2.4–3.2 ppm for the CHR–OH groups and 6.4 ppm for the COOH group.

^{13}C NMR spectra demonstrate that complexes **14E–21E** are isomerically pure in solution. The ^{195}Pt signals (2350–2627 ppm) of the complexes are observed at higher field than that of the tris(acetone) complex **1** ($\delta(^{195}\text{Pt}) = 2696$ ppm).¹⁰ Complexes with carbohydrate ligands having stronger donor sites ($3 \times \text{OH}$) give ^{195}Pt chemical shifts in the range of 2350–2560 ppm, whereas those having weaker donor sites ($2 \times \text{OH} + \text{O}_{\text{acetal}}/\text{O}_{\text{ring}}$) are in the range of 2524–2627 ppm.

3. Structural Analysis Using ^{13}C -Labeled Monosaccharide Ligands. As a consequence of the very weak donor character-

istics of neutral carbohydrate ligands, coordination-induced shifts (CIS)¹⁷ are small in the platinum(IV) complexes. For example, ^{13}C chemical shift differences between noncoordinated and coordinated carbohydrate ligands are <2 ppm and thus are unreliable diagnostic probes of the coordination mode of the carbohydrate ligands. Useful information, however, can be obtained from ^{13}C – ^{13}C and ^{13}C – ^1H spin-coupling constants, which can be measured readily in ^{13}C -labeled compounds.¹⁸

1,2-*O*-Isopropylidene- α -D-glucopyranose (**10B***) (all ^{13}C -labeled compounds are marked with an asterisk) singly labeled at each of the saccharide carbons (C1–C6) was synthesized and complexed with the trimethylplatinum cation to give ^{13}C -labeled complex **14E***. A number of J couplings involving the labeled carbons were measured, and a subset of these data are used here to illustrate their use in confirming the structure of **14E**.

a. $^1J_{\text{CC}}$. The involvement of the exocyclic C5–C6 fragment in 1,2-isopropylidene- α -D-glucopyranose in Pt(IV) complexation is confirmed by comparing $^1J_{\text{C}_5\text{C}_6}$ in **14E*** (34.4 Hz) with $^1J_{\text{C}_5\text{C}_6}$ in the noncomplexed sugar **10B*** (40.6 Hz). The large decrease in this coupling observed upon complexation is consistent with the known effect of the C–C torsion angle in vicinal diol fragments on $^1J_{\text{CC}}$; $^1J_{\text{CC}}$ is considerably smaller when the two oxygens are syn than when they are anti.¹⁸ As a control, $^1J_{\text{C}_5\text{C}_6}$ in 1,2;5,6-di-*O*-isopropylidene- α -D-glucopyranose (**1A***) (34.4 Hz) is identical to that observed in **14E***, as expected since similar constraints on the C5–C6 torsion angle are imposed by the protecting group in **1A*** and the platinum in complex **14E***. By comparison, the remaining four $^1J_{\text{CC}}$ values in **10B*** change by ≤ 2 Hz upon complexation with Pt.

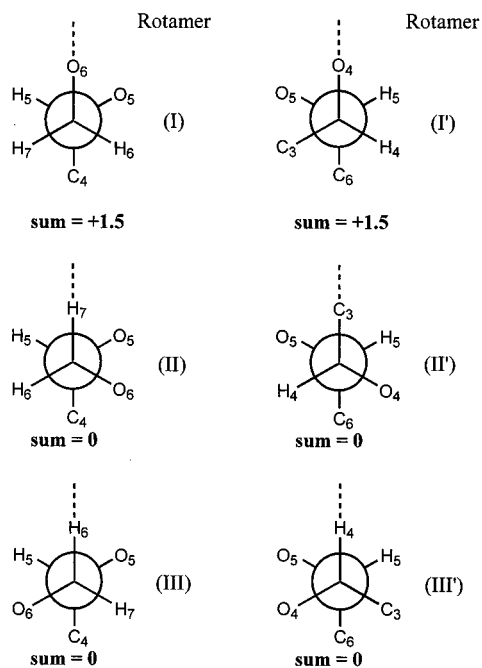
b. $^2J_{\text{CC}}$, $^3J_{\text{CH}}$, and $^3J_{\text{CC}}$. Since $^1J_{\text{C}_5\text{C}_6}$ in **14E** indicated the involvement of the C5–C6 fragment in Pt(IV) complexation, additional structural information on the complex was obtained by evaluating other J_{CC} and J_{CH} values in this region of the molecule. The geminal $^2J_{\text{C}_3\text{C}_5}$ and $^2J_{\text{C}_4\text{C}_6}$ values were interpreted using the projection resultant method.¹⁸ Newman projections and projection resultants for $^2J_{\text{C}_4\text{C}_6}$ are shown in Scheme 6. Nine combinations of rotamers are possible, leading to nine predicted values for $^2J_{\text{C}_4\text{C}_6}$. The observed $^2J_{\text{C}_4\text{C}_6}$ in **14E*** is 0 Hz, which is consistent with combinations 2, 3, 4, and 7. However, the magnitude of $^1J_{\text{C}_5\text{C}_6}$ (see above) indicates that O5 and O6 cannot be anti, excluding rotamer III, and the similar magnitudes of $^3J_{\text{H}_5\text{H}_6} = 6.2$ Hz and $^3J_{\text{H}_5\text{H}_7} = 5.7$ Hz in **14E*** exclude rotamer I, thus leaving only one combination 4 consistent with all of the available data. This geometry is also consistent with $^3J_{\text{C}_3\text{H}_5}$ (2 Hz; C3–H5 approximately anti-periplanar), $^3J_{\text{C}_4\text{H}_6}$ (3.1 Hz; C4–H6 approximately gauche), and $^3J_{\text{C}_3\text{C}_6}$ (1.7 Hz; C3–C6 approximately gauche). These J couplings involving carbon confirm that the solution structure of **14E** is similar to that observed in the crystal.⁹

4. ESI-MS Analyses. Mass spectra of the new complexes **14E–21E** were obtained by the direct injection ESI-MS technique using solutions of the pure complexes in dry acetone (Figure 1a). In all cases except **18E**, where no signal was found, the mass peaks of the molecular cations $[\text{PtMe}_3\text{L}]^+$ (L = carbohydrate) were detected, showing an isotopic envelope characteristic of monocations containing one platinum atom

(17) Ahlrichs, R.; Ballauff, M.; Eichkorn, K.; Hanemann, O.; Kettenbach, G.; Klüfers, P. *Chem. Eur. J.* **1998**, *4*, 835–844.

(18) (a) Schwarcz, J. A.; Perlin, A. S. *Can. J. Chem.* **1972**, *50*, 3667–3676. (b) Bock, K.; Pedersen, C. *Acta Chem. Scand.* **1977**, *B 31*, 354–358. (c) Bose, B.; Zhao, S.; Stenutz, R.; Cloran, F.; Bondo, B. P.; Bondo, G.; Hertz, B.; Carmichael, I.; Serianni, A. S. *J. Am. Chem. Soc.* **1998**, *120*, 11158–11173. (d) Church, T.; Carmichael, I.; Serianni, A. S. *Carbohydr. Res.* **1996**, *280*, 177–186. (e) Carmichael, I.; Chipman, D. M.; Podlasek, C. A.; Serianni, A. S. *J. Am. Chem. Soc.* **1993**, *115*, 10863–10870.

Scheme 6



combination	front pathway	back pathway	projection sum	expected coupling [Hz]
1	I	I'	+ 3.0	3
2	I	II'	+ 1.5	0
3	I	III'	+ 1.5	0
4	II	I'	+ 1.5	0
5	II	II'	0	- 2
6	II	III'	0	- 2
7	III	I'	+ 1.5	0
8	III	II'	0	- 2
9	III	III'	0	- 2

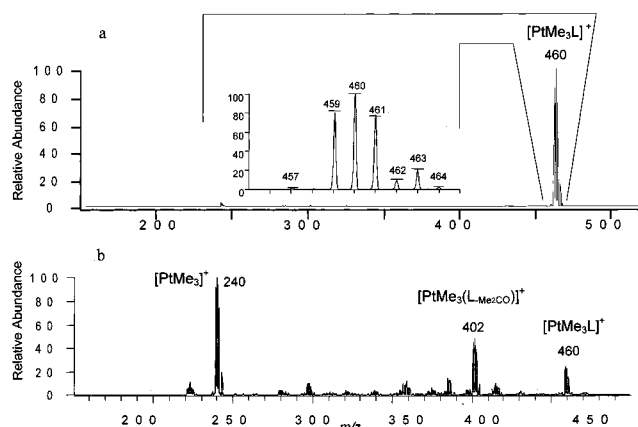
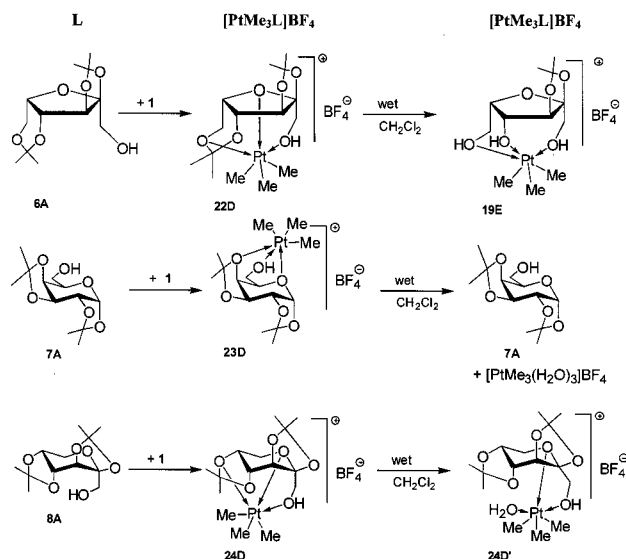


Figure 1. (a) ESI mass spectrum of $[\text{PtMe}_3\text{L}]\text{BF}_4$ (**19E**) ($\text{L} = 2,3\text{-}O$ -isopropylidene- α -L-sorbofuranose) (solvent: acetone). Full scan mass spectrum showing the molecular mass of the cation, and expanded spectrum of the $[\text{PtMe}_3\text{L}]^+$ ion at m/z 460 showing the expected intensity due to Pt isotopic composition (calculated intensities are shown by horizontal bars). (b) CID spectrum (dissociation of the parent ion at m/z 460).

[natural isotopic composition: ^{190}Pt (0.01%), ^{192}Pt (0.79%), ^{194}Pt (32.9%), ^{195}Pt (33.8%), ^{196}Pt (25.3%), and ^{198}Pt (7.2%)]. The observed isotopic patterns of the molecular cations are in good agreement with the calculated values. In most cases, the mass peaks of the ions $[\text{PtMe}_3\text{L}]^+$ represent the most intensive peaks (basis peak), but further mass peaks of platinum-containing cations such as $[\text{PtMe}_3]^+$ (m/z 240) and $[(\text{PtMe}_3)_2\text{L-H}]^+$ ($\text{L-H} =$ deprotonated carbohydrate ligand) were also detected. As the

Scheme 7



com- pound	$[\text{PtMe}_3\text{L}]\text{BF}_4$ (yield)	L
6A	22D (45%)	2,3,4,6-di- <i>O</i> -isopropylidene- α -L-sorbofuranose
7A	23D (48%)	1,2,3,4-di- <i>O</i> -isopropylidene- α -D-galactopyranose
8A	24D (62%)	2,3,4,5-di- <i>O</i> -isopropylidene- β -D-fructopyranose
	24D' (73%) ^a	2,3,4,5-di- <i>O</i> -isopropylidene- β -D-fructopyranose

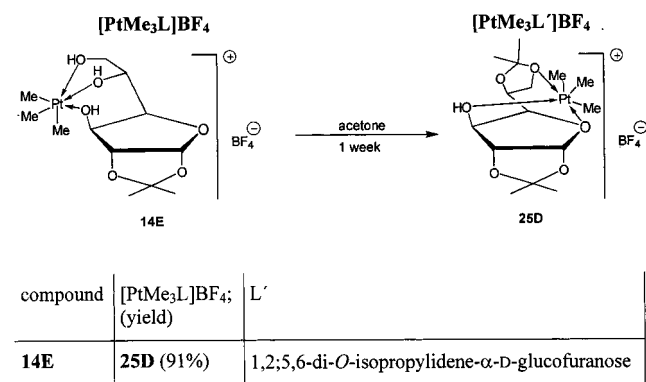
^a $[\text{PtMe}_3\text{L}(\text{H}_2\text{O})]$.

NMR data show, these species are not present in the original solution but are formed during the ionization process and/or by thermal decomposition (proven by varying the ESI spray voltage from 3.0 to 5.5 kV and the capillary temperature from 100 to 300 °C). Furthermore, collision-induced dissociation (CID) experiments (multistage mass analysis, MS^3 and MS^5) demonstrated that the molecular cations $[\text{PtMe}_3\text{L}]^+$ are not formed by fragmentation processes of higher mass.

The fragmentation processes (CID of the isolated parent ions) of the complex cations $[\text{PtMe}_3\text{L}]^+$ show a significant dependence on the coordination mode of the platinum. For complexes with monoprotected furanose ligands without coordination of the protecting group (**14E**–**17E**, **19E**, and **20E**), product ions were formed by the loss of acetone from the parent ion ($\Delta m = 58$ amu, Figure 1b). In contrast, another fragmentation process was observed for the complex **21E** in which the acetal oxygen of the protecting group participates in the coordination. In this case a daughter ion at m/z 428 ($\Delta m = 30$ amu) was detected. Using **21E** with perdeuterated methyl ligands, a daughter ion at m/z 431 ($\Delta m = 36$ amu) was observed, which proves that two methyl ligands of the platinum(IV) cation are eliminated, probably as ethane. Complex **18E** did not show any signal; facile deprotonation of the highly acidic carboxylic group apparently yields a neutral complex which is not detected by ESI-MS.

B. Platinum Complexes with Diprotected Carbohydrate Ligands. 1. Synthesis. The diprotected monosaccharides 2,3,4,6-di-*O*-isopropylidene- α -L-sorbofuranose (**6A**), 1,2,3,4-di-*O*-isopropylidene- α -D-galactopyranose (**7A**), and 2,3,4,5-di-*O*-isopropylidene- β -D-fructopyranose (**8A**) react in acetone with **1** without accompanying cleavage of an isopropylidene protecting group to yield new platinum complexes $[\text{PtMe}_3\text{L}]\text{BF}_4$ (**22D**–**24D**) ($\text{L} = \mathbf{6A}$ –**8A**) (Scheme 7). In these complexes, the carbohydrate ligands coordinate through one hydroxyl group

Scheme 8



and two weaker donors, namely, the ring oxygen of the furanose or pyranose ring and an acetal oxygen of an isopropylidene group.

These complexes exhibit a higher sensitivity to air and moisture than those where the ligand is coordinated through three hydroxyl groups. In wet methylene chloride, complex **22D** reacts with the loss of one isopropylidene group to give complex **19E** in which the monoprotected carbohydrate ligand is coordinated via three hydroxyl groups. In contrast, dissolving **23D** in wet methylene chloride results in the cleavage of the carbohydrate ligand without cleavage of a protecting group. Dissolution of **24D** in wet methylene chloride yields complex **24D'** in which the ligated acetal oxygen atom of the isopropylidene group is replaced by an aqua ligand without deprotection of the carbohydrate ligand. Thus, complex **24D'** exhibits a unique coordination mode to platinum (bidentate carbohydrate ligand).

As illustrated in Scheme 8, platinum-promoted isopropylidene represents a novel route to prepare platinum(IV) complexes with diprotected carbohydrate ligands. Within 1 week, **14E** in acetone was converted to **25D**, which was isolated in 91% yield. As found for **22D–24D**, this diprotected carbohydrate ligand exhibits an unprecedented coordination mode with two acetal oxygens and only one hydroxyl oxygen as donors.

Isopropylidene groups in complexes involving diprotected pyranose ligands (**23D**, **24D**) are cleaved more slowly in acetone than those in complexes involving diprotected furanose ligands **22D** and **25D**. Furthermore, the exocyclic isopropylidene group in complexes involving furanose ligands **22D** and **25D** exchanges in [D₆]acetone as shown by ESI-MS experiments, which proves that the platinum-promoted deprotection/protection reaction occurs at a significant rate.

The platinum–carbohydrate complexes **22D–25D** were isolated as white, air- and moisture-sensitive powders or colorless crystals (**24D'**) in moderate to good yields (45–91%), and they were fully characterized by microanalysis, ¹H, ¹³C, and ¹⁹⁵Pt NMR spectroscopy, single-crystal structure analysis (**24D'**), and ESI mass spectroscopy.

2. Crystal Structures. Slow concentration of a solution of **22D** in wet methylene chloride gave colorless crystals of complex **19E** suitable for single-crystal X-ray crystallography. Its molecular structure is shown in Figure 2, and selected bond lengths and angles are listed in Table 3. 2,3-*O*-Isopropylidene- α -L-sorbofuranose acts as a neutral tridentate ligand which is coordinated via three hydroxyl groups ($\kappa^3\text{O}^{1,4,6}$ coordination). The six-, seven-, and eight-membered 1,3,2-dioxaplatina rings exhibit boat, chair, and distorted chair conformations, respectively.

The cyclic system is not free of bond angle strain, as indicated by the O–Pt–O angles in particular. One of these angles is

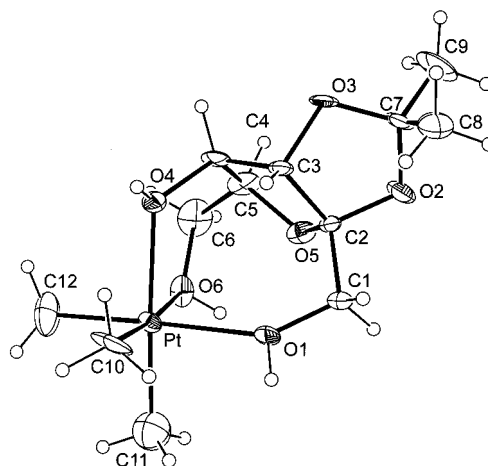


Figure 2. Molecular structure of the cation of **19E** (ORTEP-III²³ diagram displaying 30% probability ellipsoids).

Table 3. Selected Bond Lengths and Angles for **19E**

Bond Lengths (Å)			
Pt–O1	2.26(1)	C1–O1	1.43(2)
Pt–O4	2.24(1)	C1–C2	1.52(2)
Pt–O6	2.16(1)	C2–C3	1.47(3)
Pt–C10	2.10(1)	C3–C4	1.51(2)
Pt–C11	1.90(3)	C4–O4	1.41(2)
Pt–C12	2.03(2)	C5–C6	1.50(2)
Bond Angles (deg)			
O1–Pt–O4	91.2(5)	C10–Pt–C11	89.6(7)
O1–Pt–O6	95.3(5)	C10–Pt–C12	89.5(9)
O1–Pt–C10	88.3(8)	C11–Pt–C12	91(1)
O1–Pt–C11	87.6(8)	Pt–O1–C1	143.5(9)
O1–Pt–C12	177.4(7)	Pt–O4–C4	122.2(9)
O4–Pt–O6	82.5(4)	Pt–O6–C6	121(1)
O4–Pt–C10	92.9(8)	O1–C1–C2	108.2(7)
O4–Pt–C11	177.2(7)	O4–C4–C3	111.1(8)
O4–Pt–C12	90.3(8)	O4–C4–C5	111.1(7)
O6–Pt–C10	174.2(9)	O6–C6–C5	109.9(8)
O6–Pt–C11	95.1(8)	C5–O5–C2	110.7(7)
O6–Pt–C12	87.0(7)		

distinctly smaller than 90° (O4–Pt–O6 = 82.5(4)° vs O1–Pt–O6 = 95.3(5)° and O1–Pt–O4 = 91.2(5)°), whereas the C–Pt–C angles remain nearly orthogonal (89.5(9)–91(1)°). Two Pt–O bonds (O1, O4) are equal within the tolerance limit (3 σ) (Pt–O1 = 2.26(1), Pt–O4 = 2.24(1) Å) and are equivalent to those in [PtMe₃(C₉H₁₆O₆)]BF₄ (**14E**), whose structure is shown in Figure 3 for comparison.⁹ In contrast, the Pt–O bond (O6) is significantly shorter (Pt–O6 = 2.16(1) Å). The furanose ring assumes an envelope conformation in which C4 is displaced from the C5,O4,C2,C3 plane by 0.37(1) Å. A similar distortion of 0.57(2) Å but in the opposite direction is observed in the furanose ring in **14E**.⁹ A comparison of **19E** with the noncomplexed 2,3,4,6-di-*O*-isopropylidene-2-keto-L-gulonic acid (**5A**) (the most similar carbohydrate ligand whose crystal structure is known¹⁹) shows that, apart from the conformation of the exocyclic CH₂OH group, only small changes in the conformation of the carbohydrate ligand occur upon complexation. Within the furanose ring, C5 is bent toward the O5,C2,C3,C4 plane of the furanose ring, and the dihedral angle C3,C4,C5,O5 increases by 12° upon complexation.

Dissolution of **24D** in wet methylene chloride gave colorless crystals of **24D'** suitable for single-crystal X-ray crystallography. Its molecular structure is shown in Figure 4, and selected bond lengths and angles are listed in Table 4. 2,3,4,5-Di-*O*-isopropylidene- β -D-fructopyranose acts as a neutral bidentate ligand

(19) Takagi, S.; Jeffrey, G. A. *Acta Crystallogr. Sect. B* **1978**, *34*, 2932–2934.

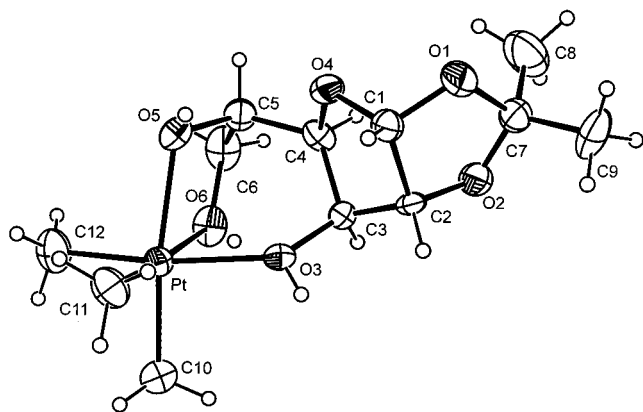


Figure 3. Molecular structure of the cation of **14E** (ORTEP-III²³ diagram displaying 30% probability ellipsoids). Selected bond lengths (Å) and angles (deg): Pt–O3 2.227(7), Pt–O5 2.24(1), Pt–O6 2.23(1), Pt–C10 2.02(1), Pt–C12 2.02(2), Pt–C13 2.07(2), O3–Pt–O5 78.6(4), O3–Pt–O6 87.5(6), O5–Pt–O6 75.7(6), Pt–O3–C3 123.5(8).⁹

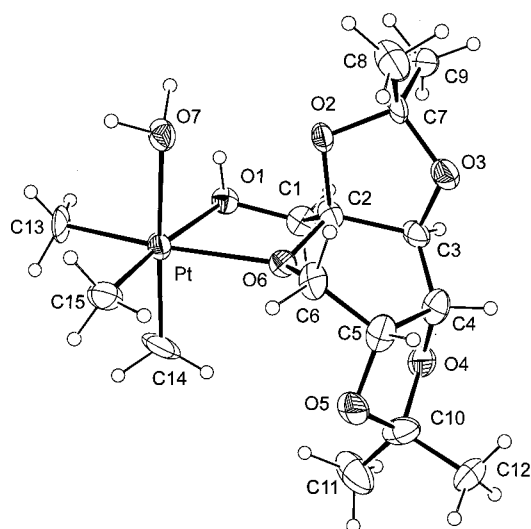


Figure 4. Molecular structure of the cation of **24D'** (ORTEP-III²³ diagram displaying 30% probability ellipsoids).

Table 4. Selected Bond Lengths and Angles for **24D'**

Bond Lengths (Å)			
Pt–O1	2.24(1)	O1–C1	1.45(2)
Pt–O6	2.26(1)	O6–C6	1.46(2)
Pt–O7	2.23(1)	C1–C2	1.50(2)
Pt–C13	2.00(2)	C2–O6	1.45(2)
Pt–C14	2.02(2)	C2–O2	1.43(2)
Pt–C15	2.00(2)	C5–C6	1.47(3)
Bond Angles (deg)			
C13–Pt–C14	90(1)	O6–Pt–C14	89.4(8)
C13–Pt–C15	88.3(9)	O6–Pt–C15	99.2(7)
C14–Pt–C15	90(1)	O7–Pt–C13	93.7(7)
O1–Pt–O6	75.3(4)	O7–Pt–C14	175(1)
O1–Pt–O7	93.1(4)	O7–Pt–C15	88.2(6)
O1–Pt–C13	95.1(8)	Pt–O1–C1	110.0(9)
O1–Pt–C14	89.9(7)	Pt–O6–C2	111(1)
O1–Pt–C15	174.2(7)	Pt–O6–C6	125.2(8)
O6–Pt–O7	87.2(4)	C1–C2–O6	105(1)
O6–Pt–C13	170.4(8)	C2–C3–C4	118(2)

which is coordinated via the hydroxyl group (O1) and the acetal oxygen atom (O6) of the pyranose ring ($\kappa^2\text{O}^{1,6}$ coordination). The coordination sphere of the platinum is completed by an aqua ligand.

The five-membered 1,3,2-dioxaplatina ring exhibits a half-chair conformation. This ring is not free of bond angle strain, which is revealed by the small O1–Pt–O6 angle (75.3(4)°),

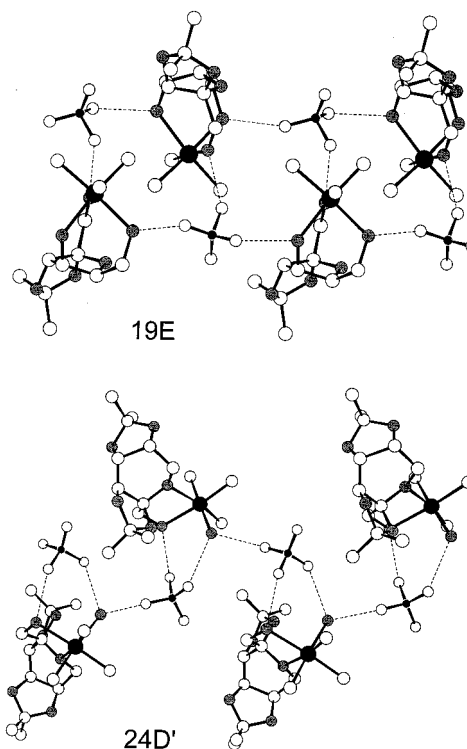


Figure 5. Unit cell structure of **19E** and **24D'**, displaying the hydrogen bonding network.

whereas the C–Pt–C angles remain nearly orthogonal (88.3(9)–90(1)°). All Pt–O bonds are equal within the tolerance limit (3σ) (Pt–O mean value 2.24 Å).

The pyranose ring of the free ligand 2,3;4,5-di-*O*-isopropylidene- β -D-fructopyranose (**8A**) exhibits a ${}^2\text{S}_0$ conformation in the solid state.²⁰ In contrast, in the crystal structure of **24D'**, the twist-boat conformation of the pyranose ring is distorted due to complexation with platinum. This distortion is caused by changes in the dihedral angles in the sugar ring; in particular, the dihedral angle C3–C4–C5–C6 is reduced by 7° and C4–C5–C6–O6 is increased by 6°.

In the crystal structures of **19E** and **24D'**, there are strong cation–anion interactions via O–H \cdots F hydrogen bonds (O \cdots F = 2.63(1)–2.70(1) Å (**19E**), 2.639(5)–2.818(5) Å) (Figure 5). In **19E**, each of the three hydroxyl groups of the carbohydrate ligand is hydrogen-bonded to a BF_4^- anion such that the crystal is threaded by double chains built up of alternating cations and anions. In **24D'**, one BF_4^- anion is hydrogen-bonded to the hydroxyl group of the carbohydrate ligand as well as to one OH group of the aqua ligand of the same cation and to a neighboring cation via the other OH group of the aqua ligand. Thus, as observed for **19E**, the crystal is threaded by chains built up of alternating cations and anions. Similar networks of O–H \cdots F hydrogen bonds were also found in **14E**⁹ and in $[\text{PtMe}_3(1,6\text{-anhydro-}\beta\text{-D-glucopyranose})]\text{BF}_4$;¹⁰ they might be essential for the marked tendency of these complexes to crystallize, which is unusual for carbohydrate–metal complexes.

3. NMR Spectroscopy. At ambient temperature, the methyl proton signals of the trimethylplatinum cation in complexes **22D**–**24D** are very broad (Table 5). This behavior may be due to different methyl shifts caused by different oxygen donors in trans positions and/or by weak coordination. In complex **24D'**, the signal is sharper and is shifted to higher field due to the

(20) Lis, T.; Weichsel, A. *Acta Crystallogr.* **1987**, *C43*, 1954–1956.

Table 5. ^1H Chemical Shifts^a of the Methyl Ligands and the Coordinated Hydroxyl Protons and ^{195}Pt Chemical Shifts for Complexes **22D**–**25D**

compd	coord mode ^b	$\delta(^1\text{H}) [^2J(\text{Pt,H})]^c$			$\delta(^{195}\text{Pt})$
		CH_3 (rt.)	CH_3 (-50°C)	OH (-50°C)	
22D	OH, O_{ring} , O_{acetal}	1.28 [74.7]	1.04 [78.8] (3H) 1.11 [78.1] (3H) 1.28 [80.4] (3H)	6.77 (1H)	2642
23D	OH, O_{ring} , O_{acetal}	1.24 [78.4]	1.10 [79.1] (3H) 1.21 [80.6] (3H) 1.27 [81.2] (3H)	6.78 (1H)	2658
24D	OH, O_{ring} , O_{acetal}	1.30 [79.4]	1.10 [78.5] (3H) 1.22 [80.9] (3H) 1.27 [80.2] (3H)	6.77 (1H)	2618
24D'	OH, O_{ring} , H_2O	1.21 [79.1]	1.04 [79.5] (6H) 1.11 [79.9] (3H)	6.66 (H_2O) 6.86 (OH)	2530
25D	OH, O_{ring} , O_{acetal}	1.27 [79.9]	1.03 [79.1] (3H) 1.09 [78.0] (3H) 1.22 [80.7] (3H)	6.91 (1H)	2600

^a In parts per million, in $[\text{D}_6]\text{acetone}$. ^b O_{ring} = furanose ring oxygen. O_{acetal} = acetal oxygen of the isopropylidene group. ^c $^2J_{\text{Pt,H}}$ values in brackets, in hertz.

replacement of the weak acetal coordination by the stronger aqua ligand. In contrast, at -50°C , the broad signal is resolved into three sharp signals flanked by platinum satellites, revealing the nonequivalence of the methyl ligands as observed in **14E**–**21E**. The methyl protons trans to an acetal oxygen are shifted downfield compared to those trans to a hydroxyl group.

Coordination-induced shifts (CIS) of the carbon-bound protons of the carbohydrate ligands are not observed as expected, taking into consideration that even stronger donating deprotonated carbohydrates do not show remarkable shifts.¹⁷ However, it should be noted that all protons of the coordinated exocyclic CH_2OH fragment in complexes **22D**–**24D'** are broadened, which might be due to unresolved $^3J_{\text{Pt,H}}$ couplings. Even at low temperature (-50°C), these couplings could not be resolved. Similar observations were made for the exocyclic carbon signals in ^{13}C NMR spectra of **22D**–**24D'**. The signals of the R– CH_2OH –Pt carbon atoms show line widths of 5–10 Hz, while the remaining carbon signals are narrower (1.2–1.5 Hz). This broadening might be caused by unresolved small $^2J_{\text{Pt,OC}}$ couplings. In related trimethylplatinum complexes, these couplings have not been observed, but $^2J_{\text{Pt,SC}}$ values have been shown to be small (1–4 Hz).²¹

The ^{195}Pt shifts (2600–2658 ppm) in complexes **22D**–**25D** (coordination mode of the carbohydrate ligand: $1 \times \text{OH} + \text{O}_{\text{ring}} + \text{O}_{\text{acetal}}$) occur at higher field compared to the tris(acetone) complex **1** ($\delta(^{195}\text{Pt}) = 2696$ ppm)¹⁰ and lower field compared to complexes in which the carbohydrate ligands are ligated through three hydroxyl groups (2350–2560 ppm; Table 2). The ^{195}Pt shift in **24D'** is found at very low field ($\delta = 2530$ ppm) due to the stronger aqua ligand.

4. ESI-MS Analyses. The constitutions of complexes **22D**–**25D** in solution were confirmed by mass spectrometry (ESI; solvent: acetone). The mass peaks of the molecular cations $[\text{PtMe}_3\text{L}]^+$ are the most intensive peaks in the spectra. As for complexes **14E**–**21E**, the cations $[\text{PtMe}_3]^+$ and $[(\text{PtMe}_3)_2\text{L-H}]^+$ were also observed due to ionization processes and/or thermal decomposition. Additionally, a cation of the type $[\text{PtMe}_3\text{L}_2]^+$ was also detected (**23D**), which was found to form by thermal decomposition (see above).

CID experiments showed that the fragmentation pathway of the molecular cations $[\text{PtMe}_3\text{L}]^+$ depends strongly on the structure of the carbohydrate ligand. The furanose derivatives

22D and **25D** show loss of $\Delta m = 30$ amu (elimination of two methyl ligands, probably as ethane) from the parent ion, while in the case of the pyranose complexes **23D** and **24D**, two fragmentation processes ($\Delta m = 30$ amu and $\Delta m = 58$ amu) compete, namely, the loss of two methyl ligands ($\Delta m = 30$ amu) and the loss of a protecting isopropylidene group ($\Delta m = 58$ amu).

Conclusions

The carbohydrate–metal complexes described in this work belong to an undeveloped class of transition metal complexes containing neutral, “purely” oxygen-bound carbohydrate ligands. These ligands are much weaker donors than deprotonated carbohydrates and carbohydrates having Lewis base anchor groups, and consequently the nearly equivalent oxygen donor atoms of the sugar produce a wide range of coordination modes in the resulting metal–carbohydrate complexes.

It has been shown that monosaccharides lacking anchor groups can be bound as chelating ligands (tri- and bidentate) through a wide range of donor sites ($3 \times \text{OH}$, $2 \times \text{OH} + \text{O}_{\text{ring}}$, $2 \times \text{OH} + \text{O}_{\text{acetyl}}$, $2 \times \text{OH} + \text{O}_{\text{acetal}}$, $1 \times \text{OH} + \text{O}_{\text{ring}} + \text{O}_{\text{acetal}}$, $1 \times \text{OH} + \text{O}_{\text{ring}}$) to a transition metal in a high oxidation state (Pt(IV)). From ^1H investigations the following order of donor ability can be derived: $3 \times \text{OH} > 2 \times \text{OH} + \text{O}_{\text{ring/acetal}} > \text{OH} + 2 \times \text{O}_{\text{ring/acetal}}$. Carbohydrates having three OH group donors can be compared in their donor ability to *facial* binding polyol ligands such as inositol.²² The carbohydrates are neither oxidized by platinum(IV) nor deprotonated (the latter occurs easily using metals in high oxidation states) upon complexation, but platinum-promoted cleavage or insertion of isopropylidene protecting groups can occur depending on steric conditions.

Crystal structures are scarce for transition metal–carbohydrate complexes. Spectroscopic investigations conducted herein (NMR, ^{13}C -labeling, ESI-MS) show that the monosaccharides coordinate to platinum(IV) in the solid state and in noncoordinating organic solvents in the same manner. The use of weakly protected monosaccharides and metal-induced liberation of hydroxyl groups may provide an avenue to explore the novel chemistry of transition metal–carbohydrate complexes and promote entry to new complexes with more complicated carbohydrate ligands such as oligosaccharides. These investigations contribute to a deeper understanding of the coordination modes of carbohydrates to transition metals, which is of general interest in biochemistry, too.

Acknowledgment. We gratefully acknowledge financial support by the Deutsche Forschungsgemeinschaft and the Fonds der Chemischen Industrie and gifts of chemicals from Degussa (Hanau) and Merck (Darmstadt). We thank Omicron Biochemicals, Inc. for financial support.

Supporting Information Available: Tables containing ESI-MS spectroscopic data (zoom scan spectral data, molecular mass peak, isotopic pattern and fragmentation) and crystal data and structure refinement, atomic coordinates and equivalent isotropic displacement parameters, bond lengths and angles, anisotropic displacement parameters, and hydrogen coordinates and isotropic displacement parameters for **19E** and **24D'**. This material is available free of charge via the Internet at <http://pubs.acs.org>.

JA9902726

(22) Hegetschweiler, K.; Ghisletta, M.; Hausherr-Primo, L.; Kradolfer, T.; Schmalte, H. W.; Kramlich, V. *Inorg. Chem.* **1995**, *34*, 1950–1953.

(23) Burnett, M. N.; Johnson, C. K. *ORTEP-III: Oak Ridge Thermal Ellipsoid Plot Program for Crystal Structure Illustrations*; Oak Ridge National Laboratory Report ORNL-6895; 1996.

(21) Appleton, T. G.; Hall, J. R. *Aust. J. Chem.* **1980**, *33*, 2387–2403.